Electromagnetic Moments of the β-Emitting Nucleus ^{16}N

K. Matsuta,[1,*] T. Miyake,[1] K. Minamisono,[1] A. Morishita,[1,†] S. Momota,[2] Y. Nojiri,[2] M. Mihara,[1] M. Fukuda,[1] K. Sato,[1] S. Y. Zhu,[1,3] H. Kitagawa,[4] H. Sagawa,[5] and T. Minamisono[1]

[1]*Graduate School of Science, Osaka University, Toyonaka, Osaka 560-0043, Japan*
[2]*Kochi Institute of Technology, Tosayamada, Kochi 782-8502, Japan*
[3]*CIAE, P.O. Box 275-50, Beijing 102413, People's Republic of China*
[4]*KEK, 1-1 Oho, Tukuba, Ibaraki 305-0801, Japan*
[5]*Center for Mathematical Sciences, University of Aizu, Fukushima 965-8580, Japan*

(Received 10 October 2000)

The nuclear magnetic dipole moment μ and electric quadrupole moment Q of the β-emitting ^{16}N($I^\pi = 2^-, T_{1/2} = 7.13$ s) nucleus have been determined for the first time by detecting its β-NMR in a MgO crystal and β-NQR (nuclear quadrupole resonance) in a TiO_2 crystal to be $|\mu| = (1.9859 \pm 0.0011)\mu_N$ and $|Q| = (17.9 \pm 1.7)$ mb, respectively. Although the prediction of μ given by the Hartree-Fock calculation agrees well with the experiment, an abnormally small effective charge for neutrons is required to account for the experimental Q.

DOI: 10.1103/PhysRevLett.86.3735 PACS numbers: 21.10.Ky, 24.70.+s, 27.20.+n, 76.60.–k

Using recently developed experimental techniques, we have precisely measured the nuclear electromagnetic moments of many short-lived nuclei located around the proton and neutron drip lines to obtain a deeper understanding of nuclear properties [1–4]. Those moments reveal new trends in nuclear shell structure especially with the extended radial distribution of the valence nucleons near the nuclear surface. As well, precise knowledge of nuclear structure is necessary for the study of in-medium effects of nucleons in the nucleus [5], since nucleons β decaying at the surface of an unstable nucleus reflect the local nucleon density [6].

Of particular interest is the nuclear structure of the ground state of the unstable nucleus ^{16}N($I^\pi = 2^-, T_{1/2} = 7.13$ s) which has a rather small one-neutron separation energy $S_n = 2.49$ MeV; the shell model predicts its simple structure as predominantly consisting of one neutron occupying the $d_{5/2}$ orbital outside the doubly closed ^{16}O core, and one proton hole in the $p_{1/2}$ orbital inside the core. A definite understanding of the ground state can be inferred from the magnetic moment μ and quadrupole moment eQ. In spite of such importance, both μ and Q are not known because of the experimental difficulties in maintaining and manipulating the spin polarization of ^{16}N in suitable implantation media for long enough periods compared with its half-life $T_{1/2} = 7.13$ s. Another difficulty is the fact that the two β-decay transitions from its ground state, i.e., $2^- \rightarrow 0^+$ and $2^- \rightarrow 3^-$, have similar decay rates with opposite signs of β-decay asymmetry factors. In the present measurements, we have overcome these difficulties by making use of information obtained in the β-NQR (nuclear quadrupole resonance) detection [1] of ^{12}N($I^\pi = 1^+, T_{1/2} = 11$ ms) implanted in a TiO_2 crystal [7], and by employing a pair of new β-ray detectors by which the two transitions were separately measured.

The present experimental method and setup were essentially similar to the previous β-NM(Q)R work on ^{12}N [1,2,7–9]. Polarized ^{16}N nuclei were produced through the ^{15}N$(d, p)^{16}$N reaction initiated with a deuteron beam of incident energy $E_d = 2.5$ MeV obtained from the Van de Graaff accelerator at Osaka University. The Ti^{15}N target was prepared by nitriding a 0.5-mm thick titanium plate in enriched $^{15}N_2$ gas at $T = 1250$ K. The ^{16}N nuclei ejected from the same surface of the target, on which the incident beam impinged, over the angular range from 22° to 38° relative to the d-beam direction were implanted into a catcher. The implantation depth of the ^{16}N in the catcher was at most 1 μm from the surface, where the density of implanted ^{16}N, 10^{12} nuclei/cm^3, was almost constant throughout the implantation range. The spin polarization of the implanted nuclei was about $P_0 = 1.5\%$ with a β-ray counting rate of $\sim 1 \times 10^4$ s^{-1} measured with a set of β-ray counters and a deuteron beam intensity of 1 μA. To maintain the polarization of ^{16}N during its flight in the vacuum and to detect its NMR after implantation into the catcher, a static magnetic field of $H_0 = 7.0$ kOe was applied parallel to the polarization.

To determine $\mu(^{16}\text{N})$, the ^{16}N nuclei were implanted into the substitutional site of O atoms in a MgO crystal of $0.5 \times 20 \times 36$ mm^3 at room temperature. Also to determine $Q(^{16}\text{N})$, the ^{16}N nuclei were similarly implanted into the substitutional site of O atoms in a tetragonal TiO_2 single crystal of $0.5 \times 20 \times 36$ mm^3, as shown in the inset of Fig. 2 (below). The other site, an interstitial site, among the two found in the ^{12}N [7] study was not used in the present study. The β-NM(Q)R effect induced by an rf magnetic field H_1 applied perpendicular to H_0 was evaluated from the change in the β-ray angular distribution. For this measurement, β rays were detected by the two sets of plastic-counter telescopes placed above and below the catcher. A new technique was devised to separately detect the β-decay asymmetries in the two transitions, i.e., a set of detectors consisted of three plastic scintillators with one β-ray energy degrader inserted between the second

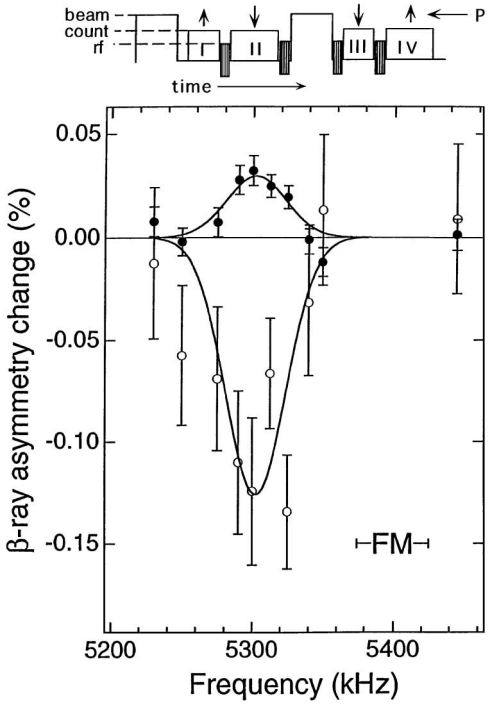

FIG. 1. A typical β-NMR (8-AP Mode) spectrum of ^{16}N implanted in cubic MgO crystals. The NMR was detected at $H_0 = 7.0$ kOe, rf $H_1 = 30$ Oe for the AFP method and at room temperature. Each rf was FM modulated 50 kHz. The inset is the time sequence program of the β-NMR using the pulsed beam method. The closed circle stands for the $2^- \rightarrow 3^-$ β decay and the open circle for the $2^- \rightarrow 0^+$.

and third scintillators. The size of each was 1 mm thick with 30×30 mm^2 area. The degrader was a 5 mm thick aluminum plate with the same area. The integrated thickness of the first two scintillators and the degrader of a set was chosen such that all the β rays from the $2^- \rightarrow 3^-$ transition with E_β(maximum) = 4.0 MeV were stopped, but the β rays, with energies higher than 4 MeV from the $2^- \rightarrow 0^+$ transition with E_β(maximum) = 10.4 MeV, penetrated the thickness and hit the third scintillator. The coincidence signals of the first and second scintillators gave 80% purity for the $2^- \rightarrow 3^-$ transition. The single counts from the third scintillator gave events $\sim$100% from the $2^- \rightarrow 0^+$ transition.

In order to measure μ, ^{16}N was produced during a beam-on production time of 8 s, followed by a beam-off time of 12.5 s for β-ray counting as shown in the inset of Fig. 1. At the end of each production time, an rf time of 20 ms duration was inserted before the next counting time started. The adiabatic fast passage technique (AFP) in NMR [10] was employed for inverting the spin polarization at the on-resonance condition. Furthermore, each counting time was divided into two with durations of 4.5 and 7.98 s. Between the two counting times, we applied again an rf for 20 ms. A pair of beam-count cyclings were repeated to observe NMR, where one cycling started with rf applied and the other started with no rf, as shown in the inset. The amplitude of each rf was constant with FM width of 50 kHz. The four up/down counting rate ratios in the two beam-count cyclings, an NMR effect of $\Delta(\mathrm{AFP}) = [(U/D)_\mathrm{I}(U/D)_\mathrm{IV}/(U/D)_\mathrm{II}(U/D)_\mathrm{III} - 1] \approx 4A(P - P_0')$ was obtained. Here, the angular distribution is given by $W(\Theta) = 1 + AP\cos\Theta$ for β rays emitted with angle Θ relative to the polarization P_0', U and D were the β-ray counts detected at $\Theta = 0°$ and 180°, respectively. The β-decay asymmetry parameters $A = -0.60$ and $+0.67$ are for the $2^- \rightarrow 0^+$ and $2^- \rightarrow 3^-$ transitions, respectively. The P and P_0' are the polarizations remaining with and without rf applied, respectively. If P_0' is completely inverted for one rf application, the maximum effect of $-8AP_0'$ is observed. Typical NMR spectra are given in Fig. 1 in which the two observed by the two transitions to 0^+ and 3^- states are clearly given. Only about $P_0' = 0.4\%$, almost $\frac{1}{4}$ of that from TiO_2, was maintained in an MgO crystal. Each sharp resonance indicates that the ^{16}N nuclei detected by the NMR were located at a symmetric site in the crystal, the substitutional site of O ions. The best fit of a Lorentzian line shape to the data gave the center frequency ν_0. The absolute value of the external magnetic field at the catcher was measured by detecting the β NMR of ^{12}N($I^\pi = 1^+, T_{1/2} = 11$ ms) implanted in the same MgO crystal and in Pt metal. By applying the diamagnetic correction for N ions in MgO crystal, $\sigma = +(355 \pm 20)$ ppm [11], we determined the μ to be $|\mu(^{16}\mathrm{N})| = (1.9859 \pm 0.0011)\mu_\mathrm{N}$ as listed in Table I.

For an electric field gradient (EFG) superposed on a high field H, the energy of the magnetic substate m of spin I is given by first order perturbation theory [12] as

$$E_m = -\mu Hm/I + (3\cos^2\theta - 1 + \eta\sin^2\theta\cos2\phi) \times \{3m^2 - I(I+1)\}eqQ/8I(2I-1). \quad (1)$$

The second derivative of the electrostatic potential evaluated along the coordinate axes which we defined as V_{ii}, where i $= x, y$, and z gives $q = V_{zz}$ and $\eta = (V_{xx} - V_{yy})/V_{zz}$, where $|V_{xx}| \le |V_{yy}| \le |V_{zz}|$. The θ and ϕ are the Euler angles between the directions of H and q which is parallel to the $\langle 110\rangle$ or $\langle 1\bar{1}0\rangle$ axis of the TiO_2 crystal. The frequency ν_m of the transition between the neighboring substates $m - 1$ and m of the spin $I = 2$ is given by

$$\nu_m = \nu_L - \nu_Q(m - \tfrac{1}{2}) \times (3\cos^2\theta - 1 + \eta\sin^2\theta\cos2\phi)/2,$$
$$\nu_Q = (\tfrac{1}{4})eqQ/h, \quad (2)$$

and $\nu_L = \mu H/Ih$ is the Larmor frequency. Previous study on ^{12}N in TiO_2 gave the EFG for N isotopes in the substitutional site of oxygen atoms as $q = \pm(198 \pm 14) \times 10^{19}$ V/m^2 and $\eta = (0.37 \pm 0.02)$ [7,9], as well as each principal component to be parallel to $\langle 110\rangle$, or $\langle 1\bar{1}0\rangle$ (V_{xx} or V_{zz}), or $\langle 001\rangle$ (V_{yy}) axes. Since we set the crystal c axis parallel to H, the two oxygen sites, one in the (0 0 1) plane in a unit crystalline cell and the other in the (0 0 $\frac{1}{2}$)

TABLE I. β-NMR detection of ^{16}N. Magnetic field (7.00 kOe) was measured by β-NMR of ^{12}N in Pt.

β transition	$2^- \rightarrow 3^-$	$2^- \rightarrow 0^+$
^{16}N resonant frequency ν_0 in MgO, (kHz)	5302.5 ± 3.2	5298.2 ± 7.6
Average	5301.6 ± 2.8	
^{12}N resonant frequency in Pt (kHz)	2441.41 ± 0.02	
g(^{12}N in Pt; uncorrected)[a]	0.457 09 ± 0.000 07	
μ(uncorrected) (μ_N)	1.9852 ± 0.0011	
Diamagnetism[b] (ppm)	+355 ± 20	
$\lvert\mu(^{16}\text{N})\rvert$ (μ_N)	1.9859 ± 0.0011	
^{12}N resonant frequency in MgO (kHz)	2438.7 ± 0.2	
Knight shift in Pt (K)	(1.1 ± 0.1) 10^{-3}	

[a]Ref. [21]. [b]Ref. [11].

plane, are all energetically equivalent for the present NQR detection.

To detect β-NQR, a set of four rf fields, ν_2, ν_1, ν_0, and ν_{-1} with rf intensity $H_1 = 10$ Oe, frequency modulation 50 kHz, and duration period 2 ms, were applied in series. The set was repeated ten times in an rf time to depolarize the initial polarization at the on-resonance condition. In the present β-NQR, no rf was applied at the middle of each count time, i.e., $2AP$ method. A pair of beam-count cyclings, one with rf on and one without rf, were repeated until we obtained enough counting statistics. Thus the NQR effect of $\Delta = [(U/D)_{\mathrm{I}}/(U/D)_{\mathrm{III}} - 1] \approx 2A(P - P_0'')$, where P_0'' is the polarization observed without rf for ^{16}N in the substitutional sites of oxygen atoms.

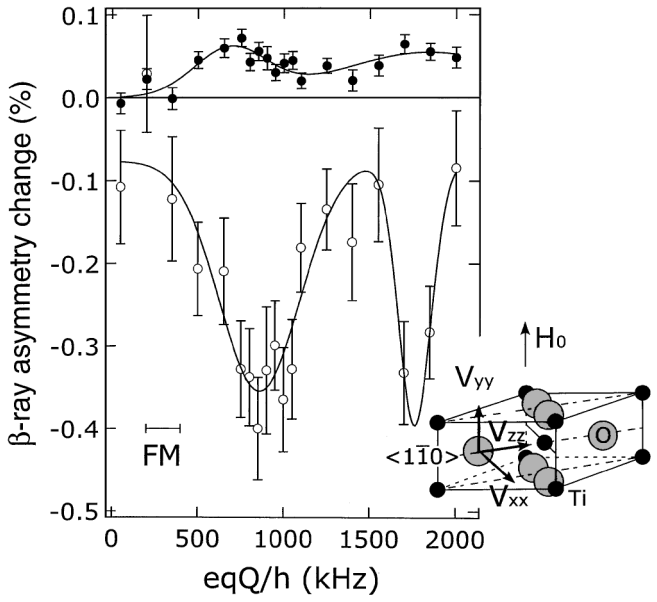

FIG. 2. Typical β-NQR spectra of ^{16}N implanted in a TiO_2 crystal detected by the depolarization method. The c axis of the crystal was set parallel to H_0 (as shown in the inset). The closed circles stand for the $2^- \rightarrow 3^-$ β decay and the open circles for the $2^- \rightarrow 0^+$. The peak at lower frequency is the normal β-NQR signal from ^{16}N at the substitutional oxygen site. The peak at higher frequency is due to the double quantum transitions between magnetic substates ± 2 and 0, the transitions of which were induced by the inner two preset rf's for an $eqQ/h \sim 1760$ kHz. The solid lines are the theoretical curves best fit to the data.

In typical spectra given in Fig. 2, two rather broad peaks are shown, where one at $eqQ/h \sim 860$ kHz corresponds to the single quantum transition of the substitutional ^{16}N, and the other at the higher $eqQ/h \sim 1750$ kHz corresponds to the double quantum transitions $\pm 2 \leftrightarrow 0$ sublevels induced by the inner two $\pm 1 \leftrightarrow 0$ transitions preset for $eqQ/h \sim 1720$ kHz. The preset ν_{-1} and ν_1, hit the true transitions ν_2(true) and ν_0(true) simultaneously. The solid curve is the theoretical β-NQR line shape best fit to the data. The results are summarized in Table II. We obtain a mean value as $|eqQ(^{16}\text{N})/h| = \{859 \pm 12(\text{stat}) \pm 13(\text{syst})\}$ kHz. The spread was $\delta eqQ/h = 150$ kHz. Taking the symmetric nature of the line shape with the present precision, we added the systematic uncertainty following the discussion in Ref. [9]. Using the known EFG [7] and $Q(^{12}\text{N})$ [9], we determined $|Q(^{16}\text{N})| = (17.9 \pm 1.7)$ mb as summarized in Table II.

Theoretical calculations of nuclear moments were carried out [13,14] by two methods with the same shell model structure factors from PSDMK interactions [15]. The first method uses the harmonic oscillator (HO) wave functions, while the modified Hartree-Fock (HF) wave functions were adopted in the second method with the halo effect. The HF calculation [13] was first carried out by solving self-consistently the HF equation for the core wave function, and then the last halo orbit is obtained to reproduce the empirical separation energy adjusting the central part of the potential.

The shell model calculation with the HO gives $\mu_{\mathrm{HO}}(^{16}\text{N}) = -2.148\mu_N$, while the HF wave function gives $\mu_{\mathrm{HF}}(^{16}\text{N}) = -2.084\mu_N$. The result with HF shows better agreement with the present experimental result $|\mu_{\mathrm{exp}}(^{16}\text{N})| = (1.9859 \pm 0.0011)\mu_N$ within a 4.7% difference. The halo effect in the theoretical predictions is very small since the radial extension is a second order effect on the magnetic moment. Also, using the effective g factors [16] obtained from the nuclei around the doubly closed shell nucleus ^{16}O, $g_\ell(n) = -0.098$ and $g_s(n) = 4.035$, we have $\mu_{\mathrm{HF}}(^{16}\text{N}$; with effective g$) = -2.100\mu_N$ to show a small change from the $\mu_{\mathrm{HF}}(^{16}\text{N})$ for which g factors of free nucleons are used. This discrepancy from experiment may indicate a necessity [13] for a higher configuration space and spin-tensor

TABLE II. β-NQR detection of ^{16}N in TiO_2. Conditions are $H_0 = 7.00$ kOe, $\nu_L = 5302$ kHz, $H_1 = \sim 10$ Oe, and frequency modulation width FM = 50 kHz. (Q.T. indicates quantum transition.)

β transition		$2^- \rightarrow 0^+$		$2^- \rightarrow 3^-$	
		Single Q.T.	Double Q.T.[a]	Single Q.T.	Double Q.T.[a]
$\lvert eqQ(^{16}\text{N in } TiO_2)/h\rvert$ (kHz)		858 ± 34	880 ± 14	683 ± 39	944 ± 120
Averaged (kHz)		877 ± 13		714 ± 37	
All Averaged	$\lvert eqQ(^{16}\text{N in } TiO_2)/h\rvert$ (kHz)	859 ± 12(stat) ± 13(syst)			
	$eqQ(^{12}\text{N in } TiO_2)/h$[b] (kHz)	469 ± 5			
	$Q(^{12}\text{N}; 1^+)$[c] (mb)	+(9.8 ± 0.9)			
	$\lvert Q(^{16}\text{N}; 2^-)\rvert$ (mb)	17.9 ± 1.7			

[a]Transition between magnetic substates $m = \pm 2 \leftrightarrow 0$. [b]Ref. [7]. [c]Ref. [9].

corrections $\mathsf{g}_p[\sigma_\times Y_2]$. But the estimated magnitudes of these corrections for the light nuclides such as ^{16}N seem to give only a slight improvement $\mu_{\text{HF}}(^{16}\text{N}$; with effective g, and $\mathsf{g}_p[\sigma_\times Y_2]) = -2.050\mu_N$, which is still insufficient to account for the present discrepancy of $\delta\mu = 0.1\mu_N$.

The theoretical single particle value for the Q moment of the $|(\pi p_{1/2})^{-1}(\nu d_{5/2})^{+1}\rangle$ configuration which occupies 96.1% of the total configuration gives $Q(^{16}\text{N}; jj) = -23$ mb, where HO with the oscillator length $b = 1.76$ fm and standard effective charges, $e_n^{\text{eff}} = +0.5e$ for neutrons in sd-shell nuclei [17] (Sagawa and Brown), are used. This is already ~30% larger than the experiment. The shell-model-code OXBASH for p- and sd-model space gives $Q_n(\text{HO}) = -47.5e_n^{\text{eff}}$ mb and $Q_p(\text{HO}) = -5.9e_p^{\text{eff}}$ using the HO wave function for proton and neutron groups, respectively, i.e., without halo effect. Using the empirical effective charges $e_n^{\text{eff}}(\text{HO}) = +0.48e$ for neutrons in sd shell and $e_p^{\text{eff}}(\text{HO}) = +1.48e$ for protons in p shell [13], the theory gives $Q(^{16}\text{N}; \text{HO}) = -31.5$ mb which is 70% larger than the experimental value. This large discrepancy may indicate a crucial effect of the small binding energy on the neutron component. On the contrary, the HF wave function with halo effect gives $Q_n(\text{HF}) = -60.4e_n^{\text{eff}}$ and $Q_p(\text{HF}) = -5.1e_p^{\text{eff}}$, to yield $Q(^{16}\text{N}; \text{HF and halo}) = -27.3$ mb by using empirical $e_p^{\text{eff}}(\text{HF}) = +1.32e$ and $e_n^{\text{eff}}(\text{HF}) = +(0.34 \pm 0.04)e$ [13]. The $Q(^{16}\text{N}$; HF and halo) is still 50% larger than the experiment. In order to reproduce the experimental value, a set of new effective charges must be introduced. Since $|Q_{\text{exp}}(^{16}\text{N})| = 17.9$ mb must be explained by the theoretical $|Q_n(\text{HF}) + Q_p(\text{HF})| = |(-60.4e_n^{\text{eff}}) + (-5.1e_p^{\text{eff}})|$, the e_n^{eff} value must be in the range of $0.19e \sim 0.21e$ for which $e_p^{\text{eff}}(\text{HF})$ is in $1.3e \sim 1.0e$. Adopting the difference of the theoretical $Q_n(\text{HF})/e_n^{\text{eff}}$ and $Q_n(\text{HO})/e_n^{\text{eff}}$ as the theoretical uncertainty for the nuclear matrix, we conclude a definitely small effective charge for the neutron in the $d_{5/2}$ state of ^{16}N, $e_n^{\text{eff}}(\text{HF}) = +(0.20 \pm 0.04)e$. The value is almost 40% of the systematic effective charges for neutrons in sd shell [13,17]. The present small $e_n^{\text{eff}}(\text{HF})$ may indicate an important effect on effective charges for loosely bound neutrons, i.e., a relatively large $\langle r^2\rangle^{1/2}$ value of them and less perturbation to the core of the nucleus. Such a small neutron effective charge may also be found in ^{15}B [18], ^{17}B, ^{18}N [19], and ^{19}O [20] provided that their nuclear structures are well investigated.

The authors express their thanks to G. F. Krebs for valuable discussions. The present work was supported by the Grant in Aid for Scientific Research and International Scientific Program given from the Japan Society for the Promotion of Science, Japan.

*Electronic address: matsuta@hep.sci.osaka-u.ac.jp
†Present address: Sumitomo Special Steel, Japan.

[1] T. Minamisono *et al.,* Phys. Rev. Lett. **69**, 2058 (1992); Nucl. Phys. **A559**, 239 (1993).
[2] K. Matsuta *et al.,* Nucl. Phys. **A588**, 153c (1995); T. Minamisono *et al.,* Phys. Lett. B **420**, 31 (1998); Phys. Lett. B **457**, 9 (1999); Phys. Lett. B **459**, 81 (1999).
[3] H. Okuno *et al.,* Phys. Lett. B **354**, 41 (1995).
[4] H. Ueno *et al.,* Phys. Rev. C **53**, 2142 (1996).
[5] D. H. Wilkinson, *Non-Nucleonic Degrees of Freedom Detected in Nuclei* (World Scientific, Singapore, 1997), p. 3; T. Minamisono *et al.,* Hyperfine Interact. **73**, 347 (1992); Nucl. Phys. **A516**, 365 (1990).
[6] K. Kubodera and M. Rho, Phys. Rev. Lett. **67**, 3479 (1991); E. K. Warburton and I. S. Towner, Phys. Rep. **243**, 103 (1994); T. Minamisono *et al.,* Phys. Rev. Lett. **82**, 1644 (1999).
[7] T. Minamisono *et al.,* Z. Naturforsch. A **53**, 293 (1998).
[8] K. Sugimoto *et al.,* J. Phys. Soc. Jpn. **21**, 213 (1966).
[9] T. Minamisono *et al.,* Phys. Lett. B **420**, 31 (1998).
[10] A. Abragam, *Principles of Nuclear Magnetism* (Oxford, New York, 1983), p. 66.
[11] F. D. Feiock and W. R. Johnson, Phys. Rev. **187**, 39 (1969).
[12] Ref. [10], p. 232.
[13] H. Kitagawa, Prog. Theor. Phys. **102**, 1015 (1999).
[14] B. A. Brown *et al.,* MSUCL Report No. 524, 1988.
[15] Preedom and Wildenthal, Phys. Rev. C **6**, 1633 (1972).
[16] T. Yamazaki, *Mesons in Nuclei* (North-Holland, Amsterdam, 1979), Vol. 2, p. 651; T. Minamisono *et al.,* Nucl. Phys. **A516**, 365 (1990); Hyperfine Interact. **73**, 347 (1992).
[17] H. Sagawa and B. A. Brown, Nucl. Phys. **A430**, 84 (1984).
[18] H. Izumi *et al.,* Phys. Lett. B **366**, 51 (1996).
[19] H. Ogawa *et al.,* Phys. Lett. B **451**, 11 (1999).
[20] T. Minamisono *et al.,* Phys. Lett. B **457**, 9 (1999).
[21] T. Minamisono *et al.,* Hyperfine Interact. **78**, 111 (1993).